J. Condensed Matter Nucl. Sci. 38 (2024) 161–170

Research Article

Deuteron Momentum and the Umweg Factor Initiate and Limit Successful CF/LANR

Mitchell R. Swartz

JET Energy, Inc., Wellesley Hills, MA, USA

Abstract

The use of dry preloaded ZrO_2PdNiD nanostructured materials in NANOR®-type components has previously demonstrated the presence of unwanted electrical avalanche behavior during successful over-driven LANR. This unwanted electrical response immediately ends the excess heat as the component returns to prosaic V*I power dissipation. This paper further examines these critical electron breakdown processes. The observed electrical breakdown in active nanostructured ZrO2PdNi LANR (lattice activated nuclear reactions) nanostructured materials and components is classically analyzed. Deuteron momentum and scattering are most important because they initiate, and then limit the success of, CF/LANR activity. We find that the deuteron momentum produces deuteron scattering, and if large enough the scattering and energy loss then limits the success of, CF/LANR activity. These collisions can create a detour ["umweg"] ruining the requisite path to deuteron synchrony needed for the desired excess heat.

Keywords: Nanor®-type components, deuteron momentum, umweg factor, successful LANR

1. Preloaded Deuterated LANR Nanomaterials

CF/LANR is very real, including with the use of dry preloaded ZrO_2PdNiD NANOR®-type components [1], [2], [3], [4]. NANOR®-type CF components have a ZrO_2-PdD or ZrO_2-PdNiD core. They are about ∼2 centimeters length, usually with ∼50-250 milligrams preloaded material. Their ability to demonstrated activity with the generation of real excess heat is easily, and repeatedly, shown (confer Figure 1).

Figure 1 shows the input electrical power to an ohmic control and then the NANOR®-type component 7–24, and the resultant output thermal power from both as a function of time. The input and output integrated energies are shown as dashed lines. The NANOR®-type component had a peak power output was ∼12.1 Watts when driven with 4 Watts. This is an incremental power gain of ∼300%, observed then the component was electrically driven below avalanche voltage [5].

2. Confirmation of Two Electrically Driven LANR States

CF/LANR is very real. The active mode is driven by the applied electric field and the enabled by the lattice vacancy-locked deuteron ions coherently interacting [6]. If adequate synchronous conditions are achieved, then cold fusion

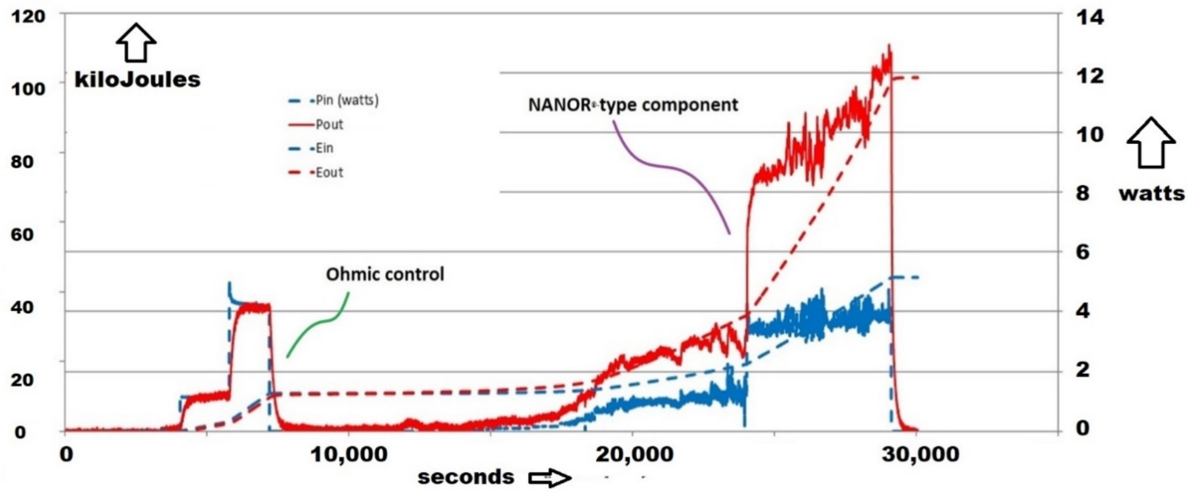

Figure 1. Calorimetry of a driven NANOR®-type component after an ohmic control to calibrate. This figure shows the input and output electrical power, and energy, to an ohmic control and then the NANOR®-type component 7–24.

(LANR) can, and does, occur. However, as shown previously, and electrically-driven LANR systems have two modes, and only one is active making the desired 'excess heat' [ref. 5; confer Figure 2]. Figure 2 presents the graphical output of a reproducible nanostructured NANOR®-type two-terminal CF electrical component, driven in both of its two different electrically driven states; and in its 'off' state and also while 'off' with an electrical ohmic control being driven. Vertical axes plot the electrical input power and the heat generated, as a function of time.

Figure 2 confirms the existence of two states. Figure 2's curves plot the temperature rise [delta-T in degrees C] of the ohmic control and the NANOR®-type LANR component, both normalized to input electrical power as a function of time so that the ratios can be used to estimate incremental power gain. There is obvious incremental power gain for the CF/LANR component until the avalanche, at which time (count ∼3700) the component has no energy gain, but has a response similar to an ohmic resistor. This also saliently demonstrates that outside of the CF/LANR active state, the component acts as any other ohmic resistor, and thus this confirms that the calorimetry was calibrated, and verifies the excess heat yet an additional way. Thus, these curves confirm the existence of two states. This result also demonstrates excess heat obtained from a Ni-D nanomaterial system, as reported previously in a high impedance aqueous CF/LANR system.

In Figure 3, the curves confirm that there are two driven LANR states, but only one (1) gives excess heat. The three modes (responses) are the undriven "off"-state, the unwanted electrical avalanche mode, and the optimal operational state, the "Desired Active Mode", where "excess" energy is being released [7], [8], [9]. Shown in Figure 3 are spectra of the same NANOR®-type CF/LANR component [NANOR® 7-6] in three different electronic states, resolved by dual wavelength coherent electric-driven volume-enhanced reflection spectroscopy.

These are the overlaid Spectra of the three Different Electronic States Optical Signatures for the same preloaded ZrO_2PdD NANOR®-type CF/LANR Component in three different electrical drive modes. The plots show the reflected optical intensity as a function of wavelength, initially from two incident coherent optical beams but also with reflected backscatter from the core along with the initial optical beams. The vertical axis represents the intensity of the returned

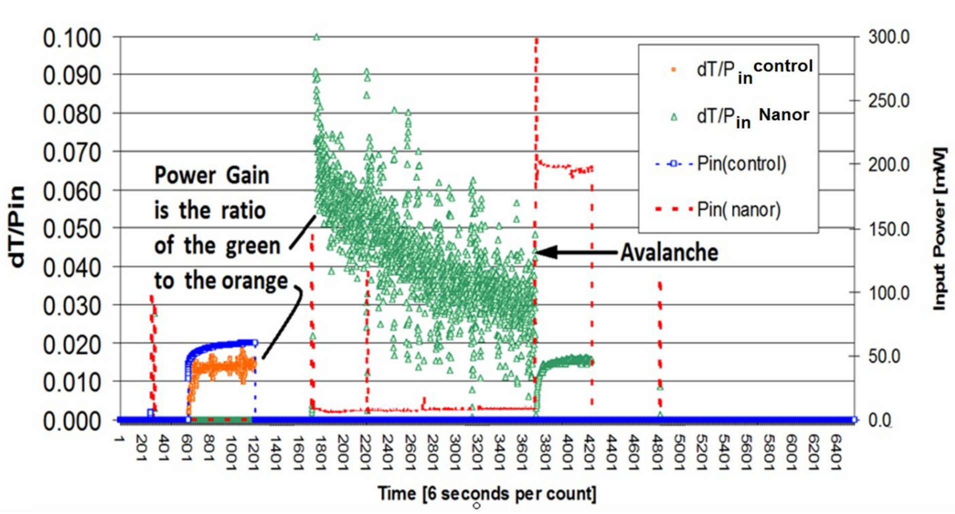

Figure 2. Demonstration of Excess Power Gain and then Sudden Loss of Activity after Electrical Avalanche for a NANOR®-type LANR component - The electrical input power and delta-T/Pin (representative of the measured instantaneous power gain) from the ohmic control and then the nanostructured two-terminal NANOR®-type ZrO_2- NiD component. The region of the Avalanche is labeled.

backscatter plotted as intensity as a function of wavelength. The horizontal axis plots the decreasing frequency to the right. The output of the first laser is shown as the peak on the left side, located at 532 nm.

3. Electrical Breakdown of Deuterated LANR Nanomaterials

When an electric field is applied, initially at low intensities, there is a region where the nanostructured LANR core acts like a very high impedance electrical resistor of several million (or several orders of magnitude higher) ohms. However, as the voltage is increased beyond a critical voltage, the electrical resistive properties of the nanostructured material core suddenly change. The component's electrical impedance post-avalanche may remain as low as only ∼8000 ohms from initially megohms to gigaohms or more.

This is a major problem for CF/LANR. Successful CF/LANR in nanomaterials is totally abolished by these electrical avalanches. In fact, this breakdown of the components resistance is what is seen above a threshold voltage. These threshold for avalanche have ranged from 30 to 1900 volts or more. Unfortunately, all ZrO_2(PdNiD) LANR nanostructured materials do, at least in some configurations, demonstrate this Zener-type avalanche behavior.

Figure 4 shows an actual avalanche electrical breakdown behavior observed in a dry preloaded, active LANR nanostructured NANOR®-type component. This occurs when the component is driven above a time-dependant threshold voltage. What is suddenly wrought is an increase of electrical current even at lower applied voltages. With the appearance of this electrical avalanche there is termination of the desired excess heat. That change with electrical avalance of the LANR component makes the component act like an ohmic resistor.

In Figure 4, note that three regions are seen; consisting of the initial plateau of electrical impedance, then the rapid fall off, and finally a sloped region at higher voltage.

Sometimes, the LANR nanomaterial electrical avalanche behavior is followed by hysteresis and partial reversibility over days. Nonetheless, optimal power gain of NANOR®-type cold fusion components is only found below the threshold breakdown.

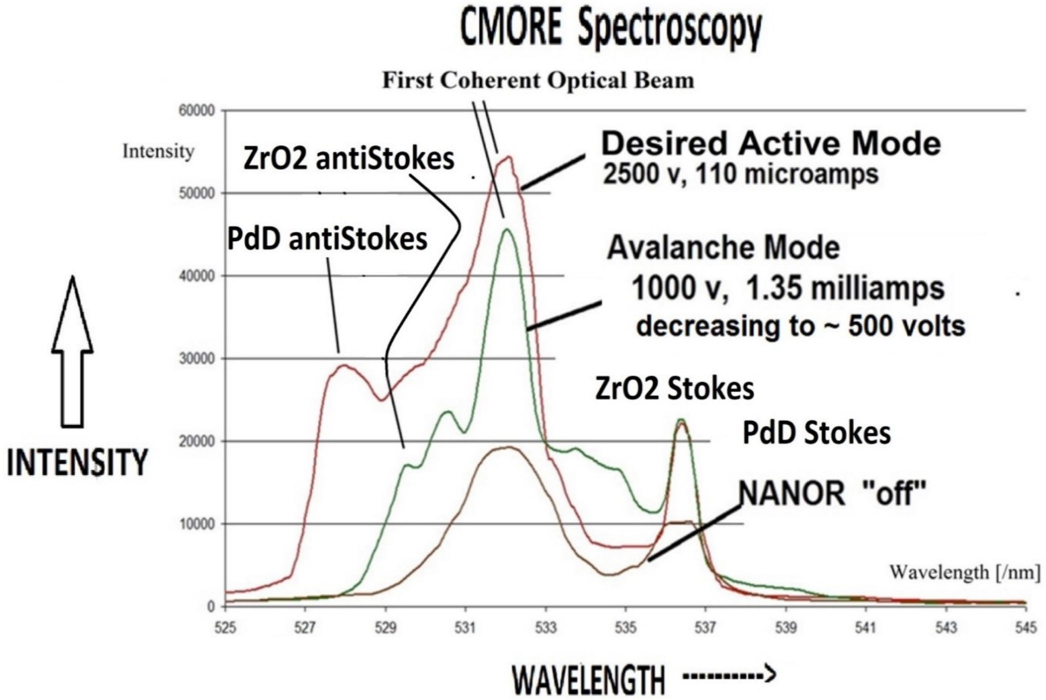

Figure 3. CMORE Spectra of ZrO_2PdD NANOR®-type CF/LANR. These are the overlaid Spectra of the three different Electronic States Optical Signatures for the same preloaded ZrO_2PdD NANOR®-type CF/LANR Component in three different electrical drive modes. Shown are spectra of the same NANOR®-type CF/LANR component [Nanor ® 7-6] in three different electronic states, resolved by dual wavelength coherent electric-driven volume-enhanced reflection spectroscopy. Labeled are the assignments of the anti-Stokes peaks to Zirconia and PdD.

Why does avalanche occur? The sudden loss of successful CF/LANR with avalanche must be better understood. In this paper, we demonstrate that it is caused by increased scattering of deuterons, producing a detour [“umweg”] in their paths. The functional result is optimal operating point (OOP) operation which has revolutionized successful CF/LANR, as shown in the graph below, and as shown by open demonstration at ICCF-10. In the next section, this breakdown will be connected to momentum and optimal operating point manifolds, which are found throughout LANR (CF/LENR/CMNS). We have generally related them to loading, and then beyond the peak to losses through unwanted pathways involving gas (D_2) evolution.

Figure 5 with its demonstration of Optimal Operating Point Operation explains many of the many “negative” results of similar systems, are the result of a failure to operate the system at the optimal operating point, which is an optimum peak in the excess heat and power gain curves as a function of input electrical power. The optimal operating point reflects the relatively narrow peak (maximum) of the biphasic production rate curve for the products obtained by the desired reactions (heat, helium-4) as a function of input electrical power [1], [2], [3], [4]. Driving with electrical input power beyond the peak optimal operating point does not improve the production of the desired product but instead yields an under desirable falloff of the production rate with increasing input power. Thus, the failure to operate similar systems at the optimal operating point, because of driving the systems inadvertently or unintentionally beyond the optimal operating point, accounts for some of the widespread difficulties in observing the desired reactions.

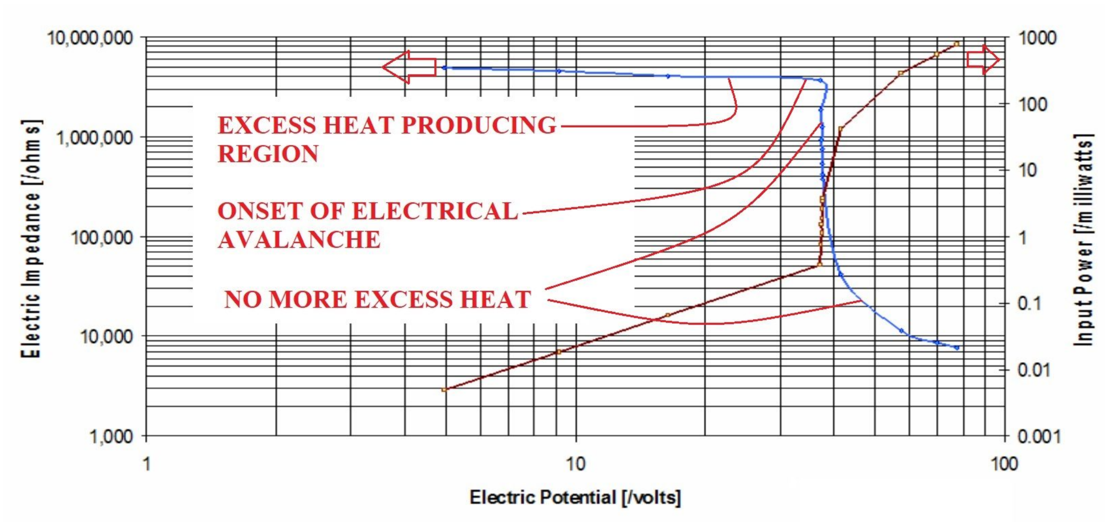

Figure 4. Impedance and Electrical current as a function of applied electric potential (volts). Shown is Avalanche (Zener-type?) Behavior in an LANR nanostructured NANOR® device containing ZrO_2(PdNiD). This figure shows the response, and particularly the Avalanche behavior with 3 distinct regions, as first observed with ZrO_2-NiH NANOR®-type component.

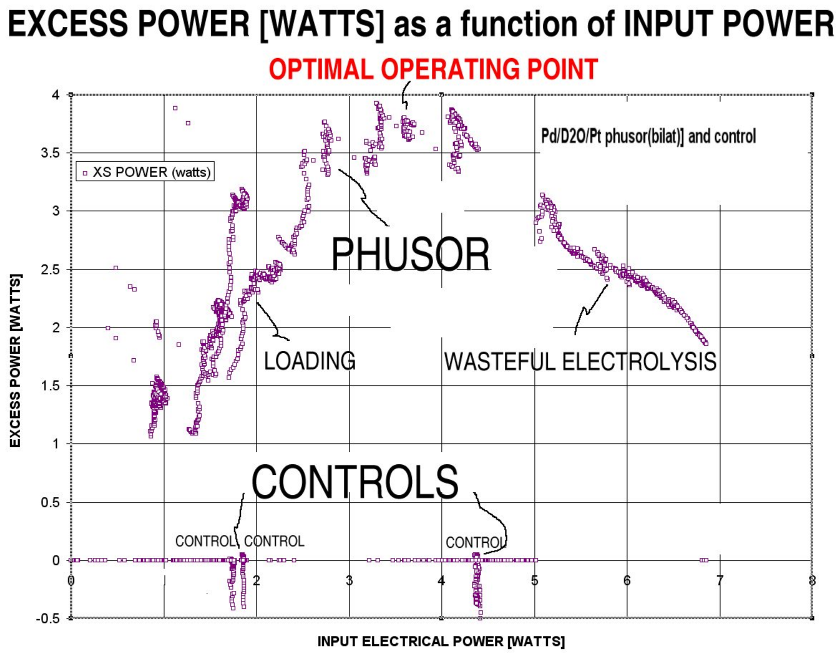

Figure 5. Optimal Operating Point Operation. The optimal operating point reflects the relatively narrow peak (maximum) of the biphasic production rate curve for the products obtained by the desired reactions (heat, helium-4) as a function of input electrical power [1], [2], [3], [4].

4. Analysis - Deuteron Momentum Initiates LANR

Deuteron momentum driven by an applied electric field first initiates, and secondary deuteron scattering then limits, active (successful) CF/LANR. These analyses of momentum and applied electrical power in LANR are important because they control LANR. Briefly, successful LANR is associated with applied electric field intensities correctly applied to loaded active palladium or nickel (or their nanostructured equivalent), followed by sustained deuteron flow through the materials, the magnitude of which can be increased by a metamaterial shape [1]. The metamaterial shape can greatly influence LANR by causing an intrapalladial current.

First, understanding how input electrical power relates to LANR is important because it dominates in the Optimal Operating Point manifolds [confer Figure 5] for all known LANR outputs in LANR including generating excess energy, tritium, and helium-4 production.

Second, it is also important to consider closer the origins, and interactions between, momentum and repeated scattering and the desired result of "excess heat". In brief summary, this analysis reveals that deuteron momentum, and then deuteron scattering, create and then limits the success of, CF/LANR activity. These collisions create a detour ["umweg"] ruining the synchrony need for the desired excess heat. With each collision, the deuteron must lose some of the energy gained from the applied electric field.

Third, the use of ZrO_2PdNi nanostructured materials has demonstrated the presence of Zener-type avalanche behavior in LANR [a]. In this paper, electrical breakdown conduction in palladium is considered in terms of the lattice during the LANR reactions, ending sometimes in electron breakdown processes.

In summary, these equations show the impact of collisions on deuteron velocity. It is noted that classical Ohm's law must fail because both the actual, and drift, velocities increase proportional to the applied E-field which further guarantees electrical avalanche.

5. Analysis - Deuteron Velocities

We next consider the movement of deuterons, and other carriers, in the loaded metal. First, let us consider the deuteron flow. Thereafter, other electrical currents involving the electrons and deuterons, and their holes, all flowing through palladium in ellipsoids related to k_B*T must be considered. These are spheroids caused by thermal background heat which are distorted by the applied electric field intensity. The quasi-1-dimensional model of isotope loading handles this and has given much success to LANR including codeposition, optimal operating points and the control of tardive thermal power. In the following, V_D is the actual velocity of a deuteron, U_D is the drift velocity of the deuteron, and τ_D is the time of free flight between collision impacts. Beginning with the Newton force equation, we can write

$$m_D \frac{d\overrightarrow{V_D}}{dt} = -q\overrightarrow{E}$$

Therefore, U_D becomes (since the drift velocity is the time averaged displacement divided by the time of flight) calculable as

$$U_D = \frac{1}{\tau_D} * \int_0^{\tau_D} \left[\frac{qE}{m_D} * t \right] dt$$

The solution of this is

$$U_D = -\frac{qE}{m_D} * \tau_D$$

Now we must consider the average number of collisions per unit length, <# collision> $_D$, which is s / $\langle \Lambda_D \rangle$.

s is the umweg (detour) factor and is the ratio of actual velocity to drift velocity.

$$< \#\text{collision} >_D = \frac{s}{\langle \Lambda_D \rangle} = \frac{V_D}{\langle \Lambda_D \rangle * U_D}$$

Therefore,

$$\tau_D = \frac{\langle \Lambda_D \rangle}{V_D}$$
$$V_D = s * U_D$$

6. Analysis - Input Electrical Power and Momentum Part 1

This is the derivation of deuteron momentum to the applied electric input power. The input power is V * I. (*****)

(***** - It is wrong to subtract the thermoneutral potential because it puts a false lower number in the denominator of a ratio used to compute putative excess power gain. It is also wrong because we have seen photographic in situ evidence of non gas evolution in early-, and mid-, loading states.)

Therefore,

$$P_{in} = V * I = qE * L * [D] * \xi_D$$

So we can compare momentum to input power as:

$$\overrightarrow{p_D} = m_D * \overrightarrow{V_D} = m_D * s * \frac{-q\overrightarrow{E}}{2 * m_D} * \tau_D$$
$$\overrightarrow{p_D} = m_D * \overrightarrow{V_D} = -s * \frac{-q\overrightarrow{E}}{2} * \tau_D$$
$$\overrightarrow{p_D} = -s * \frac{-q\overrightarrow{E}}{2} * \tau_D$$

Finally, substituting for the applied electric field intensity, and where ξ_D is the charge/deuteron.

$$\overrightarrow{p_D} = -\frac{s * \tau_D}{2L * [D] * \xi_D} * \text{Pin}$$

7. Analysis - Thermal Approximation of Velocities

In all of the time preceding, and during, LANR nuclear fusion, the energy gain per unit distance is less than $k_B * T$ so the most probable velocity is secondary to $k_B * T$.

$$\overrightarrow{\|V_D\|} = \sqrt{\frac{2 * k_B T}{m_D}}$$

One can then write the actual and drift velocities as

$$\overrightarrow{U_D} = \frac{-q}{2 * \sqrt{2 * m_D \ * k_B T}} * E = \mu_D * \overrightarrow{E}$$

In this equation, the first term of the deuteron drift velocity equation is the effective electrophoretic mobility, μ_D.

8. Analysis - Deuterium Flow Equilibrium With Collisions

Classically, with each deuteron collision, the deuteron energy loss is proportional, ℵ, to the kinetic energy.

$$\Delta\varepsilon = \aleph * 1/2 \ \ m_D * V_D^2$$

Therefore, at nanoscopic equilibrium, the deuteron energy loss per collision must balance the energy gained from the applied electric field.

$$\frac{q * E * \langle\Lambda_D\rangle}{s} = \aleph * \ 1/2 \ \ m_D * V_D^2$$

First, the equations show that in loaded ZrO2-PdNiD components because both the actual, and the drift, velocities must increase proportional to the applied E-field.

Such increasing drift velocity must herald BOTH further unwanted umweg behavior and ultimately loss of synchronization of the deuterons – seen by the observed electrical avalanche, coupled with the loss of all excess heat. One prediction of this derivation is that classical Ohm's law may fail in D-loaded ZrO_2PdNi nanostructures because both the actual, and drift, velocities must both increase proportional to the applied E=field, but at some voltage cannot, and are unable to do so. Instead there is avalanche behavior.

$$V_D = -\sqrt{\frac{\mathrm{q}\,\langle\Lambda_D\rangle\,\mathrm{E}}{m_D}} * \sqrt{\frac{2}{[\aleph * s]}}$$

$$s = \sqrt{\frac{4}{\aleph}}$$

$$= -\sqrt{\frac{\mathrm{q}\,\langle\Lambda_D\rangle\,\mathrm{E}}{m_D}} * \sqrt{\frac{2}{\aleph * s}}$$

$$U_D = \frac{1}{2 * [\aleph]^4} - * \sqrt{\frac{q * \langle\Lambda_D\rangle * E}{m_D}}$$

In fact, this is what is seen (Fig. 4). LANR nanostructured materials demonstrate Zener-type avalanche behavior in ZrO_2(PdNiD) above the threshold breakdown voltage.

9. Analysis - Effective Deuteron Temperature

We can determine the temperature of the deuterons within the palladium by considering them as a deuteron gas. The deuteron temperature, Θ_D, in eV, is a function of their kinetic energy. Therefore, it is important to consider ℵ, which is the relative energy loss of each deuteron per collision. Thus,

$$k_B * \Theta_D = 1/2 * m_D * \overrightarrow{\|V_D\|}^2 = \frac{q\,\langle\Lambda_D\rangle\,\left\|\overrightarrow{E}\right\|}{\sqrt{4\aleph}}$$

Thus, the effective deuteron temperature becomes:

$$\Theta_D = \frac{\mathrm{q}\,\langle\Lambda_D\rangle\,\left\|\overrightarrow{E}\right\|}{\sqrt{4\,\aleph} * k_B}$$

It can be seen from this equation that the deuteron temperature increases both with the magnitude of the applied electric field intensity, and the mean free path length for deuterons. It falls, however, as the square root of the proportion of energy lost per collision, $\aleph$.

Attention is directed to the fact that for aqueous CF/LANR systems, the loading equation demonstrates the importance of the ratio of organizing energy to thermal disorder. Here for nanomaterial CF/LANR systems, the ratio of organizing energy to thermal disorder for the deuterons goes as $\sqrt{4\,\aleph}$.

$$\frac{q * \left\|\vec{E}\right\| * \langle\Lambda_D\rangle}{k_B * \Theta_D} = \sqrt{4\aleph}$$

Note that first, as the ordering energy is increased, the energy goes to the lattice, increasingly as the energy loss proportion, $\aleph$, goes to, and approaches, 1.

Second, therefore, as an interesting corollary, we can explicitly determine the proportion of energy lost per collision from the accelerating E-field, using the effective deuteron temperature and the applied E field intensity.

$$\aleph = \frac{1}{2}\left[\frac{q * \left\|\vec{E}\right\| * \langle\Lambda_D\rangle}{k_B * \Theta_D}\right]$$

Note that if the lattice is active and energy is not “lost” but is gained, i.e. XSH from LANR reactions; then it is gained through phonons.

10. Conclusions

In summary, the deuteron momentum is controlled by the delivered electrical input power, and that determines whether there is successful LANR. This analysis reveals that the deuteron momentum produces deuteron scattering, and if large enough the scattering and energy loss then limits the success of, CF/LANR activity. The equations demonstrate that input electrical power correlates to deuteron momentum.

It is shown that deuteron velocities are first created by the electrical input power to the component. There are collisions. After the applied electric field intensity creates the movements of the deuterons within the component’s lattice(s), with each collision, the deuteron lose some of the energy gained from the applied electric field.

Worse, these collisions can create a detour [“umweg”] ruining the both the requisite path and deuteron synchrony needed for the desired excess heat. As a result, it is noted that ultimately classical Ohm’s law must fail because both the actual, and drift, velocities increase proportional to the applied E-field which further guarantees electrical avalanche. At a critical threshold applied voltage (which produces avalanche and ends the ‘excess heat’). The functional result is optimal operating point (OOP) operation which has revolutionized successful CF/LANR, as shown in the graph below, and as shown by open demonstration at ICCF-10 [1], [4].

Acknowledgments

The author wishes to thank Gayle Verner, Alex Frank, Andrew Meulenberg, Michael Staker, Isidor Straus, Jean-Paul Biberian, David Nagel, John Wallace, Brian Ahern, Jeff Driscoll, Peter Hagelstein, Lawrence Forsley, Louis DeChiaro, and Christy Frazier for their editorial assistance, suggestions and support; and JET Energy, Incorporated and New Energy Foundation for support.

References

[1] Swartz, M.R., “Survey of the Observed Excess Energy and Emissions In LANR”, Journal of Scientific Exploration, 23, 4, 419-436 (2009).

[2] Swartz. M., “Consistency of the Biphasic Nature of Excess Enthalpy in Solid State Anomalous Phenomena with the Quasi-1-Dimensional Model of Isotope Loading into a Material”, Fusion Technology, 31, 63-74 (1997)

[3] Swartz. M., “Codeposition Of Palladium And Deuterium”, Fusion Technology, 32, 126-130 (1997)

[4] Swartz, M., G. Verner, “Excess Heat from Low Electrical Conductivity Heavy Water Spiral-Wound Pd/D2O/Pt and Pd/D2O-PdCl2/Pt Devices”, Condensed Matter Nuclear Science, Proceedings of ICCF-10, eds. Peter L. Hagelstein, Scott, R. Chubb, World Scientific Publishing, NJ, ISBN 981-256-564-6, 29-44; 45-54 (2006).

[5] Swartz, M.R., P.L. Hagelstein, G. Verner, “Impact of Electrical Avalanche on Incremental Excess Power Gain”, ICCF-19, JCMNS, 19, (2016).

[6] Swartz, M.R., “Synchronization of Vacancy-Loaded Deuterons Enables Successful LANR Mass-Energy Transfer”, ICCF-24 (pending).

[7] Swartz, M.R., “Optical Detection of Phonon Gain Distinguishes an Active Cold Fusion/LANR Component”, JCMNS, 20, 29-53 (2016).

[8] Swartz, M.R, P.L.Hagelstein, “Increased PdD anti-Stokes Peaks are Correlated with Excess Heat Mode”, J. Condensed Matter Nucl. Sci. 24, 130-145 (2017).

[9] Swartz, M.R., “Aqueous and Nanostructured CF/LANR Systems Each Have Two Electrically Driven Modes”, J. Condensed Matter Nucl. Sci. , vol 29, 177 (2019).

[10] Swartz, M.R., “Optimal Operating Point Manifolds”, Proc. ICCF14 2, (2008), p. 639; ISBN: 978-0-578-06694-3, 639, (2010).